Pharmacogn. Res., 2027; 19(1):176-184.
https://www.phcogres.com

Original Article

Chemically Synthesized Urolithin-C Regulates Glucose Uptake in HepG2 Cells

Vani Manjappa Karadi[1,2], Manjula Mavathuru Venkatappa[3], Shivakumar Venkataramaiah[3], Sanjana Bai Shivaram Singh Mahendaranath Singh[1], Sushma Mohan[1], Ramesh Komalapura Lakshmaiah[4], Devaraja Sannaningaiah[1,3,*]

[1]Department of Studies and Research in Biochemistry, Tumkur University, Tumakuru, Karnataka, INDIA.
[2]Department of Biochemistry, Maharani Lakshmi Ammanni College for Women, Bengaluru, Karnataka, INDIA.
[3]Department of Studies and Research in Food Science and Nutrition, Tumkur University, Tumakuru, Karnataka, INDIA.
[4]Department of Home Science, Maharani's Science College for Women, Mysuru, Karnataka, INDIA.

ABSTRACT

Background: In recent years, the prevalence of diabetes has increased dramatically worldwide. Although several drugs are available for its management, their severe cytotoxic effects have created a need for safer and more effective alternatives. Urolithins (A, B, C, D, M5, M6, and M7) have gained attention due to their pharmacological potential; however, Urolithin-C remains the least studied. In our previous study, we reported the anti-inflammatory mechanism of chemically synthesized Urolithin-C. **Objectives:** In this current study, the effect of chemically synthesised Urolithin-C on glucose uptake in HepG2 cells was examined. **Materials and Methods:** The antidiabetic activity of synthetically synthesised Urolithin-Con was assessed by measuring its inhibitory effects on α-amylase, α-glucosidase, and dipeptidyl Peptidase-IV (DPP-IV), along with glucose uptake studies in HepG2 cells. **Results:** The inhibitory effect of Urolithin-C on α-amylase activity was shown by 57.14% (IC_{50}=352.69 µg/mL) and α-glucosidase activity by 64.40% (IC_{50}=296.83 µg/mL) compared with the positive control acarbose. Urolithin-C in a dose-dependent manner inhibited DPP-IV enzyme activity by approximately 68% compared with sitagliptin (72%). Molecular docking analysis of α-amylase and α-glucosidase showed binding energies of -7.7 kcal/mol and –8.2 kcal/mol, respectively with the active sites. Later, Urolithin-C enhanced glucose uptake by 58.24% in HepG2 cells after 4 hr of exposure, measured through 2-NBDG fluorescence intensity. Metformin (100 µM/mL) was used as the standard control and stimulated 64.53% by flow cytometry. **Conclusion:** Urolithin-C demonstrates promising antidiabetic potential by enhancing the activity of the antioxidant enzyme G6PD, as indicated by a cellular G6PD assay.

Keywords: α-amylase, α-glucosidase, Anti-diabetic Activity, Dipeptidyl Peptidase-IV, Urolithin-C.

Correspondence:
Dr. Devaraja Sannaningaiah[1,2]
[1]Department of Studies and Research in Biochemistry, Tumkur University, Tumkur-572103, Karnataka, INDIA.
[2]Department of Studies and Research in Food Science and Nutrition, Tumkur University, Tumakuru, Karnataka, INDIA.
Email: sdevbiochem@gmail.com
ORCID: 0000-0002-4731-7043

Received: 07-05-2026;
Revised: 19-06-2026;
Accepted: 24-08-2026.

INTRODUCTION

Diabetes Mellitus (DM) is a chronic metabolic disorder that occurs when the pancreas fails to produce sufficient insulin or when the body rejects the utilisation of produced insulin, resulting in persistent hyperglycemia. The β-cells of the pancreas secrete insulin, a peptide hormone that regulates blood glucose levels (Tafesse *et al.*, 2017). In the absence of adequate or effective insulin action, the level of blood glucose increases, leading to long term damage to the vital organs such as the heart, kidneys, eyes, nerves, and blood vessels. Hence, diabetes mellitus is a multifactorial metabolic disorder characterised by disturbances in carbohydrate, fat, and protein metabolism due to impaired insulin secretion/insulin resistance (both). It is also associated with elevated levels of oxidative stress, inflammation, and pancreatic β-cell dysfunction (Guerra *et al.*, 2021). Diabetes mellitus represents a growing global health burden, affecting over 830 million people worldwide (approximately 14% of adults), with 90-95% being Type 2 diabetes. Terrifyingly, nearly 40-45% of cases remain undiagnosed, and projections estimate that the number of affected individuals may exceed 850 million by 2050, particularly in low and middle-income countries (Yameny, 2024). Under physiological conditions, glucose homeostasis is maintained through tightly regulated insulin signalling pathways. The binding of insulin to its tyrosine kinase receptor triggers autophosphorylation and activation of insulin receptor substrates (IRS-1 and IRS-2), which subsequently stimulate the PI3K/Akt pathway. This cascade promotes glucose uptake through translocation of GLUT-4 transporters to the cell membrane and suppresses gluconeogenic gene expression (Derosa and Maffioli,

OPEN ACCESS
Manuscript TECHNOMEDIA

DOI: 10.5530/pres.20270138

Copyright Information :
Copyright Author (s) 2027 Distributed under Creative Commons CC-BY 4.0

Publishing Partner : Manuscript Technomedia. [www.mstechnomedia.com]

2012). Disruption of these pathways contributes significantly to the development of diabetes.

Currently, the management strategies include increased physical activity, weight management, balanced nutrition, and pharmacological interventions. For Type 1 diabetes, insulin therapy is essential, while Type 2 diabetes management focuses on improving insulin sensitivity and controlling postprandial hyperglycemia. One therapeutic strategy involves inhibiting the breakdown of dietary carbohydrates (starch, sugars, and fibres) into absorbable monosaccharides (Parmar *et al*., 2012; Gupta *et al*., 2009). Enzymes such as α-amylase, α-glucosidase and DPP-IV play a crucial role in carbohydrate digestion into glucose, which is then absorbed into circulation (Alberti and Zimmet, 1998). Therefore, inhibition of these enzymes delays glucose absorption and helps to reduce postprandial blood glucose levels. Acarbose, voglibose and miglitol inhibits the activity of α-amylase and α-glucosidase, while sitagliptin, vildagliptin, sitagliptin and linagliptin inhibits the activity of DPP-IV. The said inhibitors despite their glucose-regulating potential, cause gastrointestinal discomfort such as flatulence, diarrhoea, and abdominal pain due to colonic fermentation of undigested carbohydrates (Srinivasan *et al*., 2017; Kim and Egan, 2008). Consequently, there is a need for safer and more effective therapeutic alternatives (Prigeon *et al*., 2003; Ball *et al*., 2002).

Fruits such as pomegranate, berries, walnuts and almonds are the storehouse of Ellagitannins (ET), a group of polyphenolic compounds (Dall'Asta *et al*., 2015). ETs in the small intestine undergo degradation by gut microbiota into ellagic acid later converted into various forms of pharmacologically active urolithin derivatives (Leng *et al*., 2025). Among the said urolithin A and B have been extensively researched as they have been found to exhibit antioxidant, anti-inflammatory, antidiabetic and metabolic regulatory effects (García-Villalba *et al*., 2022). Urolithin A activates the AMPK pathway, improves insulin sensitivity, enhances glucose uptake in muscle and liver cells and regulates mitochondrial quality (Bai *et al*., 2017). While Urolithin B improves glucose metabolism, reduces lipid accumulation, exhibits weaker anti-inflammatory and antidiabetic activity than Urolithin A (Chen *et al*., 2024). Urolithin-C is one of the least studied metabolites of the Urolithin family. In our previous study, we reported the antioxidant and mechanism of anti-inflammatory action of chemically synthesised Urolithin-C (Manjappa *et al*., 2025). Therefore, in the present study, we made an attempt to investigate the antidiabetic potential of chemically synthesised Urolithin-C and the results are presented.

MATERIALS AND METHODS

Chemicals and reagents

α-amylase from *Aspergillus oryzae*, NaH_2PO4, Na_2HPO_4, Starch, DNS Reagent, α- glucosidase from *Saccharomyces cerevisiae*, p-Nitrophenyl-β-Glucopyranoside (pNPG), Sodium Carbonate, DPP-IV Drug discovery kit, Acarbose, HEPG2-Human hepatocellular adenocarcinoma cell line (NCCS, Pune, India), MEM-alpha medium, Fetal Bovine Serum, D-PBS, Metformin hydrochloride, DMSO, MTT, Antibiotic-Antimycotic solution-100x, Trypsin EDTA, Human Glucose-6 -Phosphate 1-dehydrogenase activity assay kit, were acquired from the Sigma Aldrich Corporation in St. Louis, Missouri, USA. Each chemical is of analytical quality.

Anti-diabetic activity

Inhibition of α-amylase activity

The activity of α-amylase was carried out using previously reported techniques (Alqahtani *et al*., 2019). Various concentrations of Urolithin-C (12.5-400 µg/mL) were used in dry test tubes and 96-well plates, respectively. The samples were preincubated with α-amylase enzyme solution (0.5%) prepared in 0.1 N phosphate buffer (pH 6.8), using a total volume of 500 µL in test tubes and 50 µL in microplate wells. The mixture was incubated at room temperature for 30 min. Following preincubation, an equal volume of 1% (w/v) soluble starch solution prepared in the same phosphate buffer (pH 6.8) was added to initiate the enzymatic reaction. The reaction mixture was further incubated at room temperature for 10 min. The reaction was terminated by adding freshly prepared 3,5-Dinitrosalicylic Acid (DNS) reagent. Subsequently, the reaction mixtures were heated in a boiling water bath at 90-95°C for 8-10 min to facilitate colour development. After cooling to room temperature, the absorbance was measured at 540 nm using a microplate reader for the 96-well format and a spectrophotometer for test tube assays. Acarbose was used as the positive control. The % inhibition (I%) was calculated by using the following formula:

$$I\,\% = \frac{(Ac - As)}{Ac} \times 100$$

Ac -absorbance of the Control, As-absorbance of the Sample.

Inhibition of α-glucosidase activity

The α-glucosidase inhibition activity was carried out through the test tube and 96-well plate method, followed by previously described methods (Alqahtani *et al*., 2019; Elya *et al*., 2012). In brief, different concentrations of Urolithin-C (12.5-400 µg/mL) in dry-cleaned test tubes and 12.5-400 µg/mL in 96-well plates were taken and pre-incubated samples with 500 µL in a test tube and 50 µL in a 96-well plate of alpha-glucosidase enzyme (0.5 U/mL prepared using 0.02 M phosphate buffer) were added and incubated for 20 min at 37°C. After that, an equal volume of the substrate p-nitrophenyl-α-D-glucopyranoside (pNPG -3 mM) was added to both and the reaction mixture was incubated for 10 minutes at 37°C. Later, 150 µL of 0.1M Na_2CO_3 in a 96-well plate and 2 mL of 0.1 M Na_2CO_3 in a test tube were added to stop the reaction. Spectrophotometric and microplate readings were taken at 405 nm. Acarbose was used as a control for the study.

The Percentage of α-glucosidase Inhibition (I%) was calculated by using the following formula:

$$I\ \% = \frac{(Ac - As)}{Ac} \times 100$$

Ac-Absorbance of the Control, As-Absorbance of the Sample.

DPP-IV Inhibition Study

The DPP-IV enzyme inhibition activity was examined as followed by the previously described method (Amin *et al*., 2019). A clean dry 96-well plate was filled with a different concentration (12.5-400 µg/mL) of Urolithin-C and 30 µL of assay buffer, followed by the addition of inhibitor sitagliptin (p32/98 standard). Then 10 µL of DPP-IV enzyme was added to the well plate, except the blank (assay buffer alone) well and the plate was incubated for 10 min at 37ºC. After preincubation, 50 µL of substrate Gly-pro-pNA was added to the well plate and the reaction mixture was kept for 30 min at 37ºC. Then the absorbance was measured at 405 nm with the help of a 96-well plate reader. The DPP-IV enzyme inhibition of Urolithin-C was calculated using the following formula:

$$\%\ \text{DPP} - \text{IV inhibition} = \frac{(\text{Abs of Control} - \text{Abs of Sample})}{\text{Abs of Control}} \times 100$$

Molecular docking

The Urolithin-C compound and protein (PDB ID: 4W93 and 3TOP) were subjected to docking using Auto Dock Vina to position them within the active region of proteins. The chemical structure of the compound was obtained from the PubChem database with appropriate 2D orientation. Additionally, the molecule's energy was minimised using ChemBio3D. The ligand molecule, which had undergone energy minimisation, was subsequently employed as input for Auto Dock Vina to conduct the docking simulation. The crystallographic structure of the receptor molecules, amylase and glucosidase (Protein Data Bank (PDB) ID: 4W93 and 3TOP), was obtained from the PDB. The structures were modified by eliminating all heteroatom coordinates and water molecules and incorporating hydrogens, Kollman charges, and the absent C-terminal oxygen. The Auto Dock 4.2 program was designed to accept only receptor files that do not contain residues with non-integral charges. Subsequently, the target protein files were generated by excluding the related residue from the protein structure using the Auto Dock 4.2 auto-preparation of target protein files (MGL tools 1.5.6) (Kajaria *et al*., 2013).

Cell Line Maintenance

The cell line HepG2 (Human hepatocellular adenocarcinoma cell line) was purchased from NCCS, Pune, India. The purchased cells were maintained in Minimum Essential Medium (MEM) with 2 mM L-glutamine and Earle's balanced salt solution contained 1.5 g/L sodium bicarbonate, 0.1 mM non-essential amino acids and 1 mM sodium pyruvate supplemented with 10% Fetal Bovine Serum (FBS) along with the 1% antibiotic-antimycotic solution maintained in the modified atmosphere with 5% CO_2 and 18-20% O_2 in the CO_2 incubator at 37ºC. After reaching 80% of density, cells were detached using 0.025% trypsin and 0.01% EDTA (in Dulbecco's Phosphate Buffered Saline) solution.

Cell viability and proliferation studies

MTT assay and cell morphological assessment

The cytotoxicity effect of Urolithin-C was measured on HepG2 cells through the MTT assay, followed by the previously published method (Odeyemi and Dewar, 2019a). In brief, 15,000 cells were plated in 200 µL of cell culture media was added to the 96-well plate and incubated at 37ºC for overnight. Later, the medium was replaced with DMEM having various concentrations of Urolithin-C (12.5-200 µg/mL). The cells were incubated for 24 hr at 37ºC with 5% CO_2 atmosphere. After the incubation, the cells were treated with 100 µL of MTT reagent (0.5 mg/mL) and incubated for 3 hr at 37ºC. Then the formed formazan crystals were dissolved in 100 µL of DMSO and it was measured at 570 nm using a microplate reader. The viability of cells treated with DMEM alone was considered 100%. The percentage cell viability was calculated using the following formula:

$$\%\ \text{cell viability} = \frac{\text{OD of treated cells}}{\text{OD of Untreated cells}} \times 100$$

The morphological changes in HepG2 cells treated with different concentrations (12.5 µg/mL to 200 µg/mL) of Urolithin-C for 24 hr at 37ºC. The treated cells were observed and recorded using an inverted biological microscope with a scale of 200 µM.

Glucose uptake study by Flow Cytometry: 2-NBDG staining

The Glucose uptake was analysed through flow cytometry by using 2-NBDG staining was carried out by using the method of Zou *et al*. (2005). Briefly, the cultured HepG2 cells were incubated in a CO_2 incubator overnight at 37ºC with a cell density of 0.5 x 106 cells/2 mL. Followed by the incubation, aspirate the spent medium and treat the cells with Urolithin-C (50 µg/mL) and metformin (100 µMol) as a positive control in 2 mL of glucose-free culture medium containing 100 µM 2-[N-(7-nitrobenz-2-oxa-1,3-diazol-4-yl) amino]-2-deoxy-D-glucose (2-NBDG) dye and keep the cells in dark conditions for 4 hr. Then removed the medium from the cells and washed the wells with Phosphate-Buffered Saline (PBS). Incubated cells at 37ºC for 3-4 min with 400 µL trypsin and cells were collected in 12 x 75 mm FACS tubes. Then, the tubes were centrifuged at 2700 RPM for 3 min at room temperature. The absorbance was measured at 540 nm.

Glucose-6 Phosphatase Dehydrogenase (G6PD) activity

The method of Li *et al*. (2013) was followed to determine the Glucose-6 Phosphatase Dehydrogenase (G6PD) activity. The cultured HepG2 cells in a 6-well plate at a density of 2 x 105

cells/2 mL were incubated in a CO_2 incubator at 37°C for 24 hr. Followed by the above said Glucose uptake study protocol up to cell harvest, later the cells were collected and lysed and the lysate was used for further analysis. The cell lysate and standard metformin were pipetted into micro wells which contained Human Glucose-6-phosphate-1-dehydrogenase, G6PD presented in the samples, were bounded by the antibodies. A biotin-labelled antibody was added and followed by the addition of Streptavidin-HRP and incubated to form a complex. After microwells were washed using PBS and substrate solution 3,3′,5,5′-Tetramethylbenzidine (TMB) was added to the microwells and the developed colour was proportional to the amount of G6PD present in the treated cells. Then, the stop solution was added to stop the reaction. The absorbance is measured at 450 nm.

Statistical Analysis

The results were statistically evaluated and provided as mean±SD. Individual parameters were compared using one-way ANOVA in GraphPad Prism 5.0 (GraphPad Software, Inc., San Diego, CA, USA). The *p*-value ($p<0.05$) was considered as significant.

RESULTS

Urolithin-C inhibited the activity of α-amylase, α-glucosidase and DPPP-IV enzymes

The inhibition of α-amylase and α-glucosidase enzymes against the Urolithin-C was evaluated by test-tube and 96-well plate methods. Urolithin-C against the α-amylase and α-glucosidase in the test tube method showed a significant antidiabetic effect in a dose-dependent manner. In α-amylase, Urolithin-C inhibited 80.95% and the IC_{50} value was found to be 8.65 µg/mL. On the other hand, inhibition of α-glucosidase enzyme activity by Urolithin-C was found to be 78.1% with an IC_{50} value of 17.52 µg/mL. For both the enzyme activities, acarbose was used as a positive control drug and it was showed 86.76 % in α-amylase and 83.83% of inhibition in α-glucosidase (Figures 1A and 1B). Furthermore, the same enzymatic study was carried out by the 96-well plate method interestingly, it showed a satisfactory antidiabetic effect by inhibiting the α-amylase and α-glucosidase enzymes in a dose-dependent manner. About 57.14% of α-amylase inhibition was observed with an IC_{50} value of 352.69 µg/mL. The positive control acarbose showed about 98.62% inhibition with an IC_{50} value of 20.67 µg/mL (Figure S1A). On the other hand, Urolithin-C showed 64.40% of α-glucosidase inhibition with an IC_{50} value of 296.83 µg/mL, whereas about 97.81% α-glucosidase inhibition was examined in case of positive control acarbose with an IC_{50} value of 24.49 µg/mL (Figure S1B). In addition, Urolithin-C inhibited Dipeptidyl peptidase-IV (DPP-IV) activity in a dose dependent manner. Urolithin-C showed 68% DPP-IV inhibition with an IC_{50} value of 242.46 µg/mL Sitagliptin was used as a standard drug, showed 72% of inhibition (Figure 1C).

Urolithin-C interacts with histidine, aspartic acid, glutamic acid and arginine present in the active site of α-amylase, while

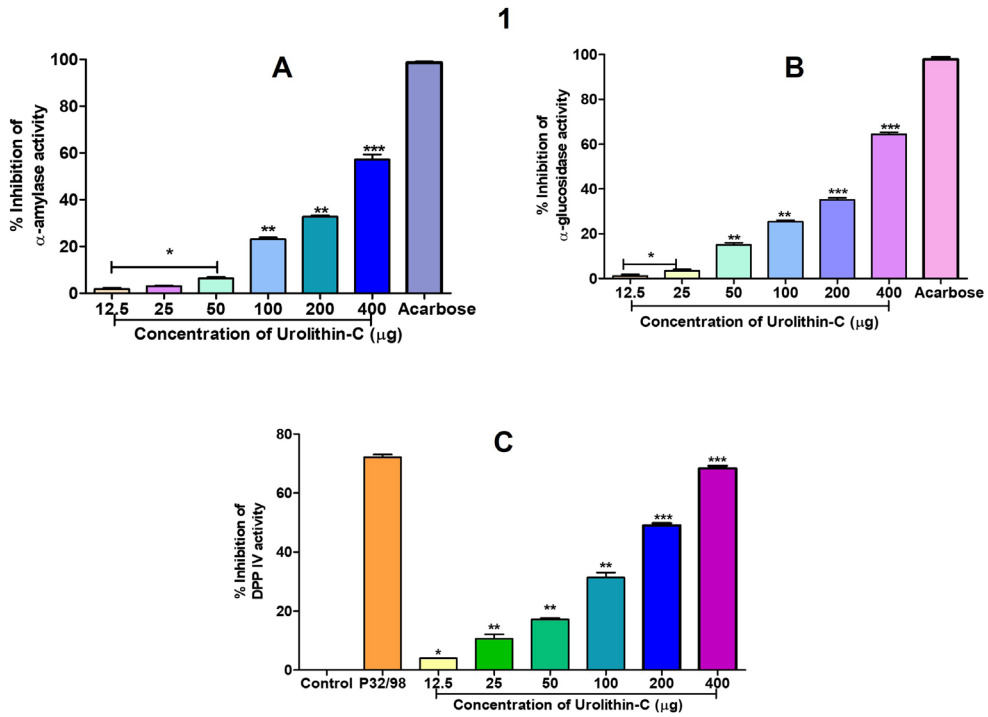

Figure 1: Inhibitory Effect of Urolithin-C on (A) α-amylase, (B) α-glucosidase, and (C) DPP-IV enzymes. The results are presented as mean±SEM ($n=3$). Significance * at $p\leq0.05$, ** at $p\leq0.01$ and *** at $p\leq0.001$.

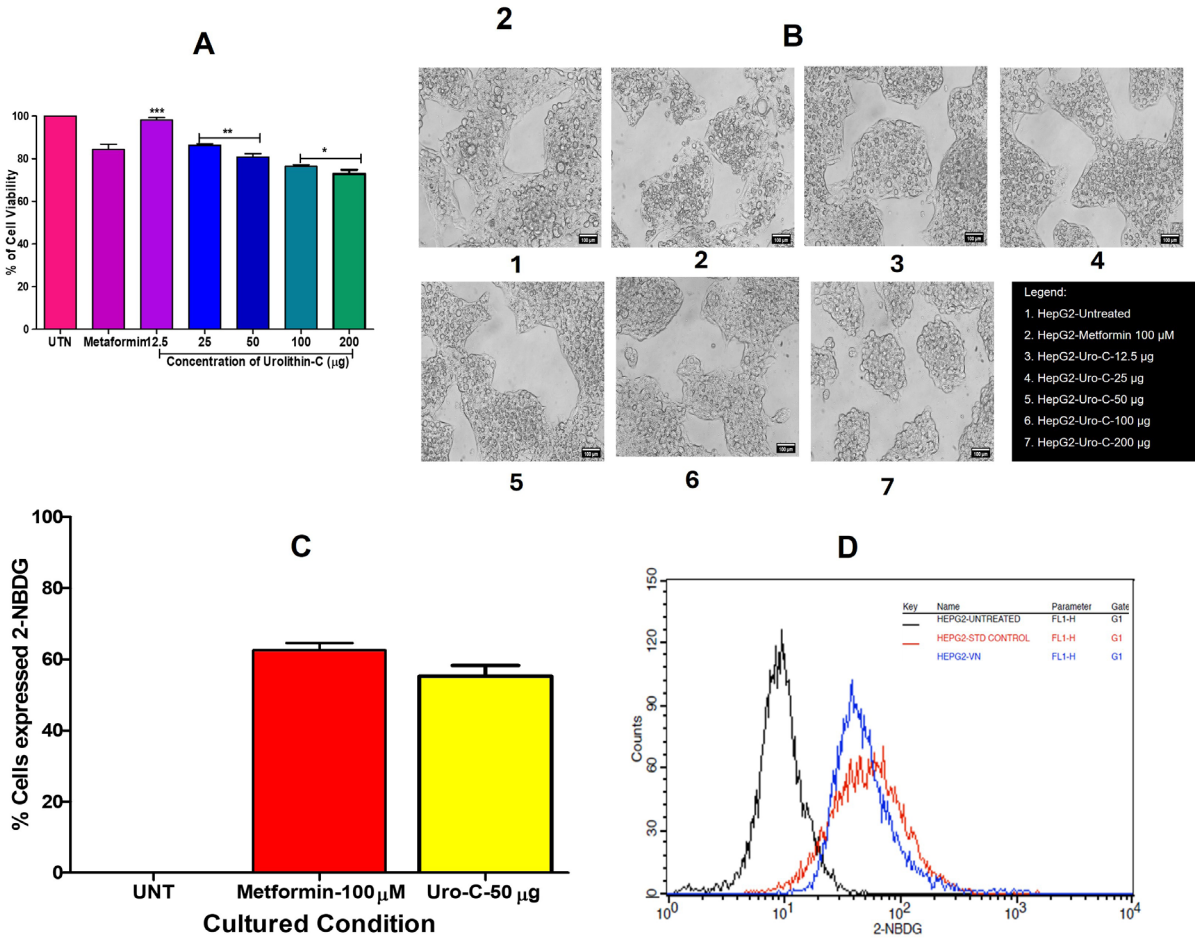

Figure 2: (A) Cytotoxic effect of Urolithin-C on HepG2 cells. (B) An inverted biological microscope was used to view cell morphology. 200 µm is the scale bar. Role of Urolithin-C on Glucose uptake by Flow Cytometry (C) % of cells expressed 2-NBDG, (D) Histogram represented the cell count in untreated, positive control metformin and Urolithin-C. The results presented are expressed as mean±SEM (n=3). Significance * at $p \leq 0.05$, ** at $p \leq 0.01$ and *** at $p \leq 0.001$.

glutamic acid and leucine are present in the α-glucosidase active site.

The interaction between the enzyme and inhibitor was investigated using molecular docking techniques. Urolithin-C showed binding energies of -7.7 kcal/mol and -8.2 kcal/mol when interacting with α-amylase and α-glucosidase, respectively (Figures S2 and S3). Urolithin-C engaged with the conserved amino acid residues HISA:101, ASPA:197, GLUA:233, ARGA:195 at the active site via hydrogen bonding of α-amylase enzyme, (GLUA:1284, LEUA:1291 of α-glucosidase interactions with the ligand Urolithin-C.

Urolithin-C exhibits a moderate cytotoxic effect on HepG2 cell lines

The cytotoxic effect of Urolithin-C on HepG2 cells was analysed by the MTT assay. The Urolithin-C was moderately toxic against the HepG2 cells, with the % cell viability of 72.85 % at the higher dose of 200 ug/mL after 24 hr of incubation. Metformin (100 µM) was used as a standard control against HepG2 cells, which showed 84.32 % viability. Based on the obtained cytotoxic results, 50 µg/mL was used for further mechanistic studies (Figure 2A). Furthermore, the morphological analyses of Urolithin-C-treated HepG2 cells were observed using an inverted microscope with a scale of 200 µM. While Urolithin-C at a greater concentration (200 µg/mL) had a smaller round body and a lower density in the treatment group, the morphology of HepG2 cells in the untreated group and metformin revealed a high density with adherent cell colonies (Figure 2B).

Urolithin-C significantly enhances glucose uptake in HepG2 cells

The role of Urolithin-C on glucose uptake in HepG2 cells was examined using 2-NBDG (2-(N-(7-Nitrobenz-2-oxa-1,3-diazol-4-yl) Amino)-2-Deoxyglucose), a fluorescent glucose analog. In case of untreated cells, 2-NBDG uptake was not noticed, suggesting the low basal glucose transport activity (Figure 2C). However, metformin-treated cells showed augmented glucose uptake with nearly about 65% of cells exhibiting positive 2-NBDG fluorescence. Similarly, in the case of Urolithin-C-treated HepG2

cells, there was an increase in glucose uptake, attainment nearly about 58%, slightly lower than the Metformin-treated group. In addition, flow cytometric analysis (Figure D) authenticated the observed results as well as untreated HepG2 cells showed a left-shifted peak, revealing low fluorescence intensity with least glucose uptake. On the hand, both Metformin and Urolithin-C treated cells displayed a rightward shift in fluorescence intensity, suggesting augmented accumulation of intracellular 2-NBDG. In comparison, metformin showed a prominent shift rather than Urolithin-C. Figure 3A indicates the dot plots of 2-NBDG fluorescence versus Side Scatter Signal (SSC). Relatively less 2-NBDG uptake was noticed in the case of untreated HepG2 cells as a lower fluorescence region was noticed. On the other hand, a moderate rise in fluorescence intensity was observed in Metformin, a standard drug treated cells. Interestingly, Urolithin-C treated cells showed rightward shift suggesting the enhanced uptake of 2NBDG. Figure B indicates the Forward Scatter (FSC) versus SSC plots endorsing uniform cell populations and proper gating across all experimental groups. Cells were distributed inside the gated region, consistently revealed the noticed difference in fluorescence was not due to a difference in cell size or granular nature rather the change in glucose uptake. Figure C represents the histogram overlays of quantitative glucose uptake distribution (2-NBDG fluorescence). Lower fluorescence intensity peak was noticed in the case of untreated group, while the positive control treated group displayed a shift towards higher fluorescence. Most importantly, the Urolithin-C-treated group showed a rightward shift in the histogram peak was observed suggesting the augmented buildup of 2-NBDG.

Urolithin-C enhances cellular antioxidant defense by upregulating G6PD activity

To ensure the cellular antioxidant potential of Urolithin-C, its effect on glucose-6-phosphate dehydrogenase (G6PD) activity was analysed (Figure 4). Basal G6PD level was found to be 8-9 ng/mL, however, metformin (Positive control) significantly raised the

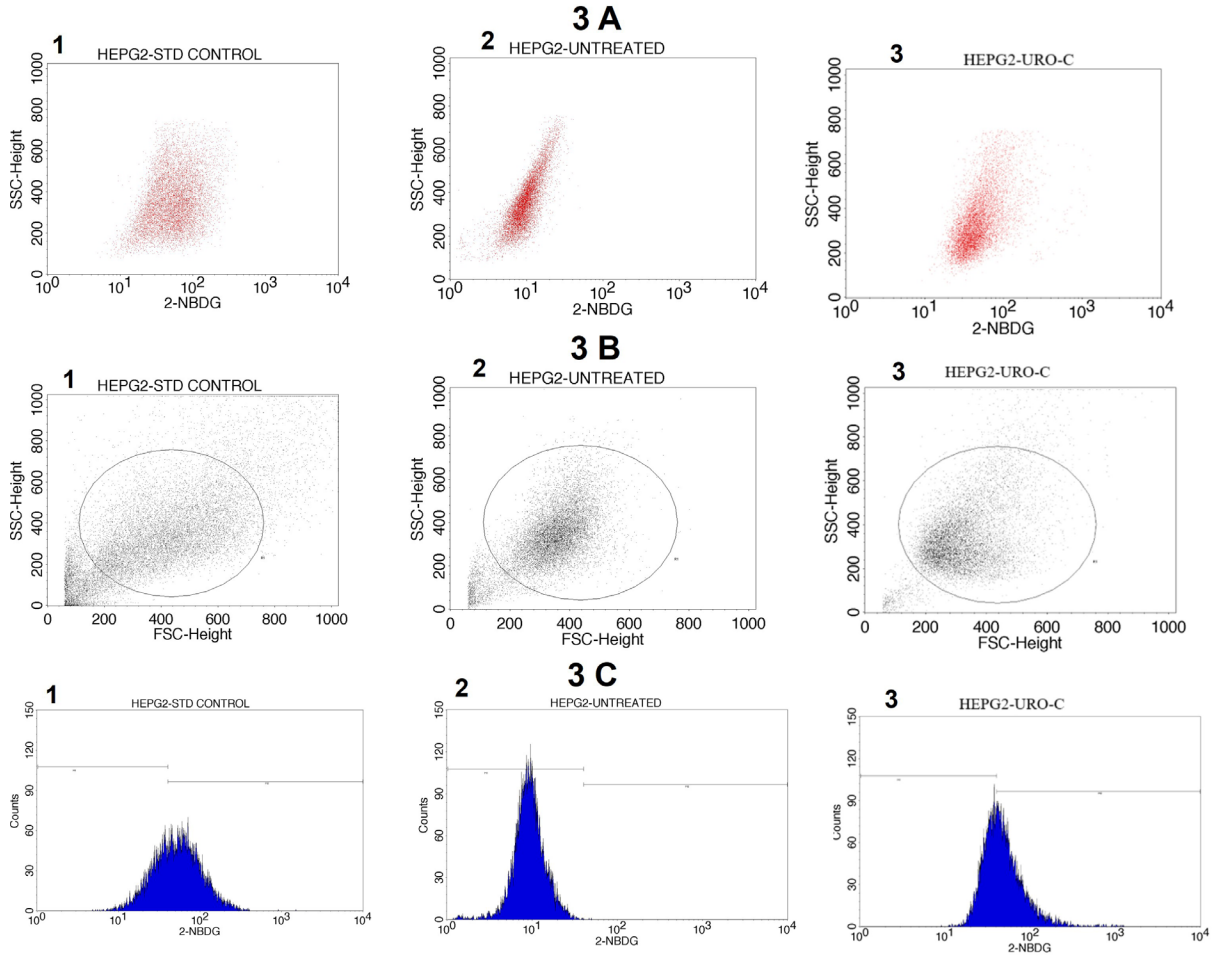

Figure 3: Glucose uptake study of the Urolithin-C against the HepG2 cells using 2-NBDG. (A) Fluorescence intensity (2-NBDG and PI, respectively) of cells. (A1) cells treated with positive standard control, (A2) untreated cells, (A3) cells treated with Uro-C. (B) Flow cytometry dot plots of 2000 cells. Different patterns of 2D plots indicating the relative size (Forward Scatter-FSC), relative granularity or internal complexity (Side Scatter-SSC) and relative FL1. (C) 2-NBDG histograms of the gated HepG2 singlets distinguish cells at the M1 and M2 phases. (Here, M1 refers to the negative expression region and M2 refers to the Positive expression region). Gating of M1 and M2 phases is approximate and can be refined using software (Cell Quest Software, Version 6.0) analysis. % cells expressed in the M2 region were considered for the study.

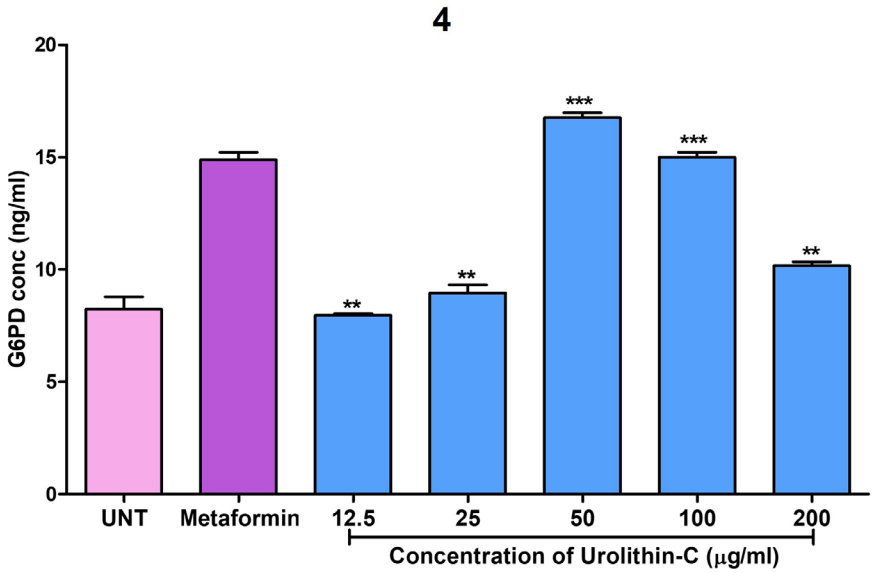

Figure 4: Effect of Urolithin-C on cellular oxidant enzyme G6PD. The results presented are expressed as mean±SEM (n=3). Significance * at $p \leq 0.05$, ** at $p \leq 0.01$ and *** at $p \leq 0.001$.

level of G6PD (15 ng/mL), suggesting the increased activity of the antioxidant enzyme. Urolithin-C modulated the G6PD activity in a dose dependent manner. At the concentration of 12.5 and 25 µg/mL, the level of G6PD was found to be increased (8-9 ng/mL), suggesting a significant improvement in comparison to the untreated group. Furthermore, at a concentration of 50 µg/mL of Urolithin-C, a marked increase in G6PD was observed (16-17 ng/mL), which was highly significant (p<0.001) compared with the metformin-treated group. However, at the concentration of (100 µg/mL) the level of G6PD was slightly lesser than 50 µg/mL. Most importantly, at the concentration of 200 µg/mL of Urolithin-C, the level of G6PD activity was significantly declined to ~10 ng/mL. These findings suggest that Urolithin-C through its antioxidant property, upregulates the activity of G6PD. The maximum effect was noticed at the concentration of 50 µg/mL. While declaimed activity at higher concentration (200 µg/mL) could be a possible biphasic effect dependent on the concentration.

DISCUSSION

The increasing frequency of diabetes mellitus globally opened the new avenues for the search for much safer yet effective therapeutic agents. Urolithins, a class of gut microbiota derived metabolites of ellagitannins, have been receiving significant evidence due to their immense pharmacological properties. Despite various types of Urolithins such as Uro-A, Uro-B, Uro-C, Uro-D, Uro-M5, Uro-M6 and Uro-M7 have been reported so far only Urolithin A and B have been extensively studied (Uzar *et al.*, 2012). While Urolithin-C is a least explored member of this family which has emerged as a promising therapeutic agent. In our previous study we reported the antioxidant and mechanism of anti-inflammatory action of chemically synthesised Urolithin-C (Manjappa *et al.*, 2025). In the current study, we examined the antidiabetic property of Urolithin-C, emphasising its capability to curb key carbohydrate-metabolising enzymes and to increase glucose uptake efficiency.

Diabetes mellitus characterised by elevated blood glucose levels, impaired insulin signalling, oxidative stress, and altered hepatic glucose metabolism (Unger and Parkin, 2010). Digestive enzymes such as α-amylase and α-glucosidase play critical roles in maintaining glucose homeostasis and are directly involved in postprandial hyperglycemia. Complex carbohydrates (polysaccharides such as starch) are first hydrolysed into oligosaccharides by α-amylase, and subsequently α-glucosidase converts carbohydrate intermediates into absorbable glucose units (Alam *et al.*, 2022). Therefore, inhibition of these enzymes slows carbohydrate digestion and reduces intestinal glucose absorption. Interestingly, Urolithin-C exhibited fair inhibitory activity against both α-amylase and α-glucosidase similar to the standard inhibitor acarbose. These findings are consistent with previous reports describing the inhibitory potential of polyphenolic compounds such as ferulic acid, coumarin, 3-isopropylcatechol, and caffeine against carbohydrate-digesting enzymes (Odeyemi and Dewar, 2019b; Zhao *et al.*, 2015).

In addition, the inhibitory effect of Urolithin-C on α-amylase and α-glucosidase was more authenticated by the molecular docking studies. The Urolithin-C showed a binding energy of -7.7 kcal/mol and -8.2 kcal/mol when it interacted with the α-amylase and α-glucosidase, respectively. Furthermore, Urolithin-C showed significant inhibition of Dipeptidyl Peptidase-IV (DPP-IV) enzyme that regulates the incretin signalling pathway. DPP-IV degrades incretin hormones including Glucagon-Like Peptide-1 (GLP-1) and Gastric Inhibitory Polypeptide (GIP), which enhance glucose-dependent insulin secretion and suppress glucagon

release. Inhibition of DPP-IV is known to lower glucagon levels, delay gastric emptying, and promote insulin secretion (Alongi and Anese, 2018). Notably, Urolithin-C exhibited 68% DPP-IV inhibition compared to standard drug sitagliptin (P32/98) 72% inhibition was noticed; hence this indicated the substantial inhibitory effect on diabetes-associated enzymes.

Additionally, to assess cellular toxicity and metabolic competence of Urolithin-C was evaluated using an *in vitro* hepatic cell model (HepG2 cells). These cells are widely used to study hepatic glucose metabolism. The MTT assay was demonstrated that Urolithin-C exhibited only moderate cytotoxicity within the tested concentration range, suggesting good biocompatibility and preservation of mitochondrial function. Morphological analysis was further confirmed normal cellular architecture with moderate apoptosis. Then followed Glucose uptake was assessed using 2-NBDG staining, a fluorescent deoxyglucose analogue that enables detection of intracellular glucose uptake. 2-NBDG uptake is directly proportional to cellular glucose transport and is mediated by Sodium-Glucose Transporters (SGLTs) and Glucose Transporters (GLUTs), allowing evaluation of compounds targeting glucose uptake and glycolysis (Langley *et al.*, 2007; Domínguez-Avila *et al.*, 2017). Measuring glucose uptake is an important approach to determine the therapeutic effects of treatments for diabetes and cancer. Reduced insulin-stimulated glucose uptake is associated with type 2 diabetes, whereas elevated glucose uptake reflects increased glycolytic activity commonly observed in cancer cells (Rena *et al.*, 2017). Untreated cells showed minimal 2-NBDG fluorescence, whereas Urolithin-C treatment significantly enhanced glucose uptake by 58.24%, compared to 64.53% observed with the standard drug metformin in HepG2 cells.

additionally, the antioxidant potential of urolithin-c was examined through analysis of Glucose-6-Phosphate Dehydrogenase (G6PD) activity. Glucose-6-phosphate dehydrogenase (G6PD) is the first and rate-limiting enzyme of the pentose phosphate pathway, generating ribose-5-phosphate and NADPH. NADPH is the principal intracellular reductant required for antioxidant defence and other reductive biosynthetic processes. Reduced G6PD activity increases cellular vulnerability to oxidative damage due to diminished NADPH availability (Viollet *et al.*, 2012; Reyes *et al.*, 2025). In the high-glucose-induced model, Urolithin-C significantly enhanced G6PD activity, thereby reducing oxidative stress and demonstrating additional antidiabetic potential. In conclusion, the potent antidiabetic effect was observed in the synthetic compound Urolithin-C and this study can attribute to multitargeted mechanisms involving in the inhibition of metabolic enzymes.

CONCLUSION

The antidiabetic activity was observed in the current study appears to arise from a synergistic, multi-targeted mechanism involving inhibition of carbohydrate-hydrolysing enzymes, suppression of DPP-IV activity, enhancement of hepatic glucose uptake, preservation of mitochondrial viability, and modulation of redox-sensitive metabolic pathways. Such a comprehensive mode of action is particularly advantageous in the management of type 2 diabetes mellitus, a complex disorder characterised by the simultaneous dysregulation of multiple pathological pathways. These findings indicate that Urolithin-C possesses considerable potential as a therapeutic antidiabetic agent; nevertheless, further molecular-level investigations and well-designed *in vivo* studies are essential to validate its efficacy and establish its clinical applicability.

ACKNOWLEDGEMENT

The authors express their sincere gratitude to Tumkur University for supporting the conduct of this research work.

ABBREVIATIONS

Uro-C: Urolithin-C; **DM:** Diabetes mellitus; **DPP-IV:** Dipeptidyl peptidase-IV; **ET:** Ellagitannins; **IRS-1:** Insulin receptor substrate 1; **IRS-2:** Insulin receptor substrate 2; **PI3K:** Phosphoinositide 3-kinase; **Akt:** Protein kinase B; **GLUT-4:** Glucose transporter type 4; **DNS:** 3,5-dinitrosalicylic acid; **pNPG:** p-nitrophenyl-α-D-glucopyranoside; **NCCS:** National Centre for Cell Science; **MEM:** Minimum Essential Medium; **FBS:** Fetal Bovine Serum; **D-PBS:** Dulbecco's Phosphate Buffered Saline; **DMSO:** Dimethyl sulfoxide; **MTT:** 3-(4,5-dimethylthiazol-2-yl)-2,5-diphenyltetrazolium bromide; **EDTA:** Ethylenediaminetetraacetic acid; **G6PD:** Glucose-6-phosphate dehydrogenase; **2-NBDG:** 2-[N-(7-nitrobenz-2-oxa-1,3-diazol-4-yl)amino]-2-deoxy-D-glucose; **PDB:** Protein Data Bank; **TMB:** 3,3′,5,5′-Tetramethylbenzidine; **SSC:** Side Scatter Signal; **FSC:** Forward Scatter; **GLP-1:** Glucagon-like peptide-1; **GIP:** Gastric inhibitory polypeptide; **SGLTs:** Sodium-glucose transporters; **GLUTs:** Glucose transporters; **GLU:** Glutamic acid; **LEU:** Leucine; **HIS:** Histidine; **ASP:** Aspartic acid; **ARG:** Arginine.

CONFLICT OF INTEREST

The authors declare that there is no conflict of interest.

REFERENCES

Alam, S., Sarker, M. M. R., Sultana, T. N., Chowdhury, M. N. R., Rashid, M. A., Chaity, N. I., Zhao, C., Xiao, J., Hafez, E. E., Khan, S. A., & Mohamed, I. N. (2022). Antidiabetic phytochemicals from medicinal plants: Prospective candidates for new drug discovery and development. Frontiers in Endocrinology, 13, 800714. https://doi.org/10.3389/fendo.2022.800714

Alberti, K. G., & Zimmet, P. Z. (1998). Definition, diagnosis and classification of diabetes mellitus and its complications: Part 1. Diagnosis and classification of diabetes mellitus provisional report of a WHO consultation. Diabetic Medicine, 15(7), 539-553. https://doi.org/10.1002/(SICI)1096-9136(199807)15:7

Alongi, M., & Anese, M. (2018). Effect of coffee roasting on *in vitro* α-glucosidase activity: Inhibition and mechanism of action. Food Research International, 111, 480–487. https://doi.org/10.1016/j.foodres.2018.05.061

Alqahtani, A. S., Hidayathulla, S., Rehman, M. T., ElGamal, A. A., Al-Massarani, S., *et al.* (2019). Alpha-amylase and alpha-glucosidase inhibition and antioxidant potential of 3-oxolupenal and katononic acid isolated from *Nuxia oppositifolia*. Biomolecules, 10(1), 61. https://doi.org/10.3390/biom10010061

Amin, M. S., Saputri, F. C., & Mun'im, A. (2019). Inhibition of dipeptidyl peptidase 4 (DPP-4) activity by some Indonesian edible plants. Pharmacognosy Journal, 11, 231–236. https://doi.org/10.5530/pj.2019.11.36

Bai, X., Yang, P., Zhou, Q., Cai, B., Buist-Homan, M., *et al.* (2017). The protective effect of hesperetin against fulminant hepatitis *in vivo* and *in vitro*. British Journal of Pharmacology, 174(1), 41-56. https://doi.org/10.1111/bph.13645

Ball, S. W., Bailey, J. R., Vogels, C. M., & Westcott, S. A. (2002). A fluorescent compound for glucose uptake measurements in isolated rat cardiomyocytes. Canadian Journal of Physiology and Pharmacology, 80(3), 205-209.

Chen, P., Zhang, X., Liu, Y., *et al.* (2024). Urolithin B protects mice from diet-induced obesity, insulin resistance, and intestinal inflammation by regulating gut microbiota composition. Food & Function, 15(14), 7518-7533.

Dall'Asta, M., Bayle, M., Neasta, J., Scazzina, F., Bruni, R., *et al.* (2015). Protection of pancreatic β-cell function by dietary polyphenols. Phytochemistry Reviews, 14(6), 933-959. https://doi.org/10.1007/s11101-015-9429-x

Derosa, G., & Maffioli, P. (2012). α-Glucosidase inhibitors and their use in clinical practice. Archives of Medical Science, 8(5), 899-906.

Domínguez-Avila, J. A., Rodrigo-García, J., González-Aguilar, G. A., & de la Rosa, L. A. (2017). Antidiabetic mechanisms of polyphenols related to increased GLP-1 and insulin signaling. Molecules, 22(6), 903.

Elya, B., Basah, K., Mun'im, A., Yuliastuti, W., Bangun, A., *et al.* (2012). Screening of α-glucosidase inhibitory activity from plants of Apocynaceae, Clusiaceae, Euphorbiaceae and Rubiaceae. Journal of Biomedicine and Biotechnology, 2012(1), 281078.

García-Villalba, R., Selma, M. V., Espín, J. C., & Tomás-Barberán, F. A. (2022). Urolithins: A comprehensive update on their metabolism, bioactivity, and associated gut microbiota. Molecular Nutrition & Food Research, 66(21), 2101019. https://doi.org/10.1002/mnfr.202101019

Guerra, J. V., Dias, M. M., Brilhante, A. J., Terra, M. F., Garcia-Arevalo, M., *et al.* (2021). Multifactorial basis and therapeutic strategies in metabolism-related diseases. Nutrients, 13(8), 2830. https://doi.org/10.3390/nu13082830

Gupta, R., Walunj, S. S., Tokala, R. K., Parsa, K. V. L., Singh, S. K., *et al.* (2009). Emerging drug candidates of dipeptidyl peptidase IV inhibitor class for the treatment of type 2 diabetes. Current Drug Targets, 10(1), 71-87.

Kajaria, D., Tripathi, R., Tripathi, J., Tripathi, Y. B., & Tiwari, S. (2013). *In vitro* α-amylase and glycosidase inhibitory effect of ethanolic extract of antiasthmatic drug Shirishadi. Journal of Advanced Pharmaceutical Technology & Research, 4(4), 206-209. https://doi.org/10.4103/2231-4040.121415

Kim, W., & Egan, J. M. (2008). The role of incretins in glucose homeostasis and diabetes treatment. Pharmacological Reviews, 60(4), 470-512. https://doi.org/10.1124/pr.108.000604

Langley, A. K., Suffoletta, T. J., & Jennings, H. R. (2007). Dipeptidyl peptidase IV inhibitors and the incretin system in type 2 diabetes mellitus. Pharmacotherapy, 27(8), 1163-1180.

Leng, P., Wang, Y., & Xie, M. (2025). Ellagic acid and gut microbiota: Interactions and implications for health. Food Science & Nutrition, 13(4), e70133.

Li, G. Q., Kam, A., Wong, K. H., Zhou, X., Omar, E. A., Alqahtani, A., Li, K. M., Razmovski-Naumovski, V., & Chan, K. (2013). Herbal medicines for the management of diabetes. In S. I. Ahmad (Ed.), Diabetes: An old disease, a new insight (Vol. 771, pp. 396–413). Springer. https://doi.org/10.1007/978-1-4614-5441-0_17

Manjappa, V. K., Venkatappa, M. M., Urs, D., Basavarajaiah, S. M., Venkataramaiah, S., Mahendranathsingh, S. B., Mohan, S., Pushpavathi, H., Krishnappa, D., & Sannaningaiah, D. (2025). Urolithin-C suppresses inflammation by blocking NF-κB signaling pathway in LPS-induced RAW 264.7 macrophages. Journal of Inflammation Research, 18, 12463–12483. https://doi.org/10.2147/JIR.S539273

Odeyemi, S., & Dewar, J. (2019a). *In vitro* antidiabetic activity affecting glucose uptake in HepG2 cells following exposure to extracts of *Lauridia tetragona*. Processes, 8(1), 33.

Odeyemi, S., & Dewar, J. (2019b). Repression of acetaminophen-induced hepatotoxicity in HepG2 cells by polyphenolic compounds from *Lauridia tetragona*. Molecules, 24(11), 2118.

Parmar, H. S., Jain, P., Chauhan, D. S., Bhinchar, M. K., Munjal, V., *et al.* (2012). DPP-IV inhibitory potential of naringin: An *in silico*, *in vitro* and *in vivo* study. Diabetes Research and Clinical Practice, 97(1), 105-111. https://doi.org/10.1016/j.diabres.2012.02.011

Prigeon, R. L., Quddusi, S., Paty, B., & D'Alessio, D. A. (2003). Suppression of glucose production by GLP-1 independent of islet hormones: A novel extrapancreatic effect. American Journal of Physiology-Endocrinology and Metabolism, 285(4), E701-E707. https://doi.org/10.1152/ajpendo.00024.2003

Rena, G., Hardie, D. G., & Pearson, E. R. (2017). The mechanisms of action of metformin. Diabetologia, 60(9), 1577-1585.

Reyes, J. S., Fuentes-Lemus, E., Fierro, A., Rivero-Rodríguez, K., Arenas, F., Davies, M. J., & López-Alarcón, C. (2025). Inactivation of human glucose 6-phosphate dehydrogenase (G6PDH) by peroxyl radicals is strongly modulated by its substrate and cofactor. Free Radical Biology and Medicine, 233, 55–69. https://doi.org/10.1016/j.freeradbiomed.2025.03.030

Srinivasan, B. T., Jarvis, J., Khunti, K., & Davies, M. J. (2008). Recent advances in the management of type 2 diabetes mellitus: A review. Postgraduate Medical Journal, 84(996), 524-531.

Tafesse, T. B., Hymete, A., Mekonnen, Y., & Tadesse, M. (2017). Antidiabetic activity and phytochemical screening of extracts of the leaves of *Ajuga remota Benth* on alloxan-induced diabetic mice. BMC Complementary and Alternative Medicine, 17(1), 243. https://doi.org/10.1186/s12906-017-175

Unger, J., & Parkin, C. G. (2010). Type 2 diabetes: An expanded view of pathophysiology and therapy. Postgraduate Medicine, 122(3), 145-157.

Uzar, E., Alp, H., Cevik, M. U., Fırat, U., Evliyaoglu, O., *et al.* (2012). Ellagic acid attenuates oxidative stress and improves brain histopathology in streptozotocin-induced diabetic rats. Neurological Sciences, 33(3), 567-574.

Viollet, B., Guigas, B., Sanz Garcia, N., Leclerc, J., Foretz, M., *et al.* (2012). Cellular and molecular mechanisms of metformin: An overview. Clinical Science, 122(6), 253-270.

Yameny, A. A. (2024). Diabetes mellitus overview 2024. Journal of Bioscience and Applied Research, 10(3), 641-645.

Zhao, D.-G., Zhou, A.-Y., Du, Z., Zhang, Y., Zhang, K., & Ma, Y.-Y. (2015). Coumarins with α-glucosidase and α-amylase inhibitory activities from the flower of Edgeworthia gardneri. Fitoterapia, 107, 122–127. https://doi.org/10.1016/j.fitote.2015.10.012

Zou, C., Wang, Y., & Shen, Z. (2005). 2-NBDG as a fluorescent indicator for direct glucose uptake measurement. Journal of Biochemical and Biophysical Methods, 64(3), 207-215.

Cite this article: Karadi VM, Venkatappa MM, Venkataramaiah S, Singh SBSSM, Mohan S, Lakshmaiah RK, *et al*. Chemically Synthesized Urolithin-C Regulates Glucose Uptake in HepG2 Cells. Pharmacog Res. 2027;19(1):176-84.

SUPPLEMENTARY DATA

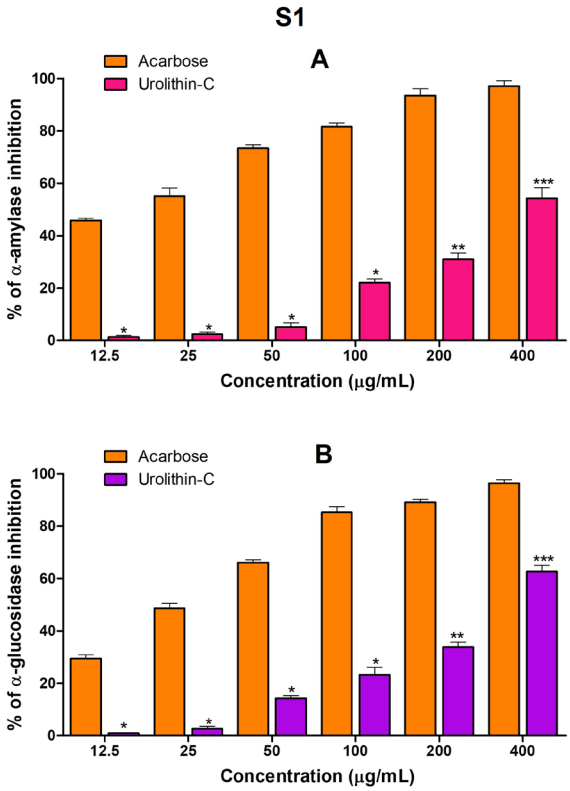

Figure S1: Inhibitory Effect of Urolithin-C on (A) α-amylase and (B) α-glucosidase on a 96-well plate, compared with Acarbose as a reference standard drug. The results are expressed as mean±SEM (n=3). Significance * at $p \leq 0.05$, ** at $p \leq 0.01$ and *** at $p \leq 0.001$.

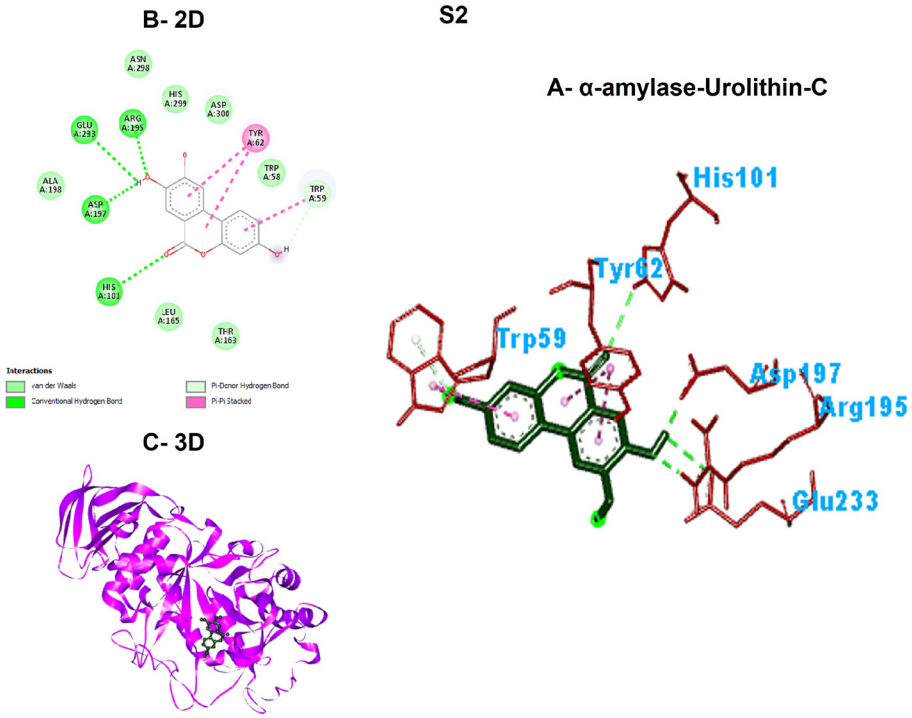

Figure S2: α-amylase - Urolithin-C interaction studies by molecular docking: (A) α-amylase - Urolithin-C Binding, (B) 2D, (C) 3D image of binding of Urolithin-C on protein through hydrogen bonding (HISA:101, ASPA:197, GLUA:233, ARGA:195) to inhibit the action of protein with a docking score of -7.7 kcal/mol.

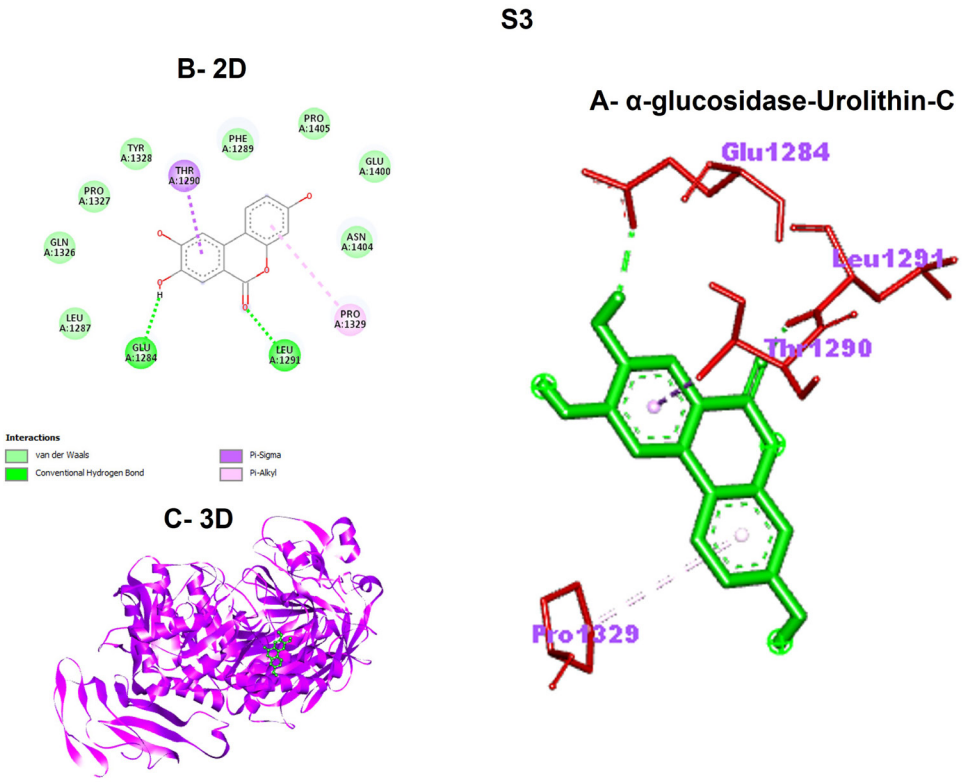

Figure S3: α-glucosidase - Urolithin-C interaction studies by molecular docking: (A) α-glucosidase - Urolithin-C Binding, (B) 2D, (C) 3D image of binding of Urolithin-C on protein through hydrogen bonding (GLUA:1284, LEUA:1291) to inhibit the action of protein with a docking score of -8.2 kcal/mol.